ACS APPLIED MATERIALS & INTERFACES

www.acsami.org

Research Article

Daylight-Induced Antibacterial and Antiviral Cotton Cloth for Offensive Personal Protection

Peixin Tang, Zheng Zhang, Ahmed Y El-Moghazy, Nicharee Wisuthiphaet, Nitin Nitin, and Gang Sun*

Cite This: *ACS Appl. Mater. Interfaces* 2020, 12, 49442–49451

Read Online

ACCESS | Metrics & More | Article Recommendations | Supporting Information

ABSTRACT: Cotton fabrics with durable and reusable daylight-induced antibacterial/antiviral functions were developed by using a novel fabrication process, which employs strong electrostatic interaction between cationic cotton fibers and anionic photosensitizers. The cationic cotton contains polycationic short chains produced by a self-propagation of 2-diethylaminoehtyl chloride (DEAE-Cl) on the surface of cotton fibers. Then, the fabric (i.e., polyDEAE@cotton) can be readily functionalized with anionic photosensitizers like rose Bengal and sodium 2-anthraquinone sulfate to produce biocidal reactive oxygen species (ROS) under light exposure and consequently provide the photo-induced biocidal functions. The biocidal properties of the photo-induced fabrics (PIFs) were demonstrated by ROS production measurements, bactericidal performance against bacteria (e.g., *E coli* and *L. innocua*), and antiviral results against T7 bacteriophage. The PIFs achieved 99.9999% (6 log) reductions against bacteria and the bacteriophage within 60 min of daylight exposure. Moreover, the PIFs showcase excellent washability and photostability, making them ideal materials for reusable face masks and protective suits with improved biological protections compared with traditional PPE. This work demonstrated that the cationized cotton could serve as a platform for different functionalization applications, and the resulting fiber materials could inspire the development of reusable and sustainable PPE with significant bioprotective properties to fight the COVID-19 pandemic as well as the spread of other contagious diseases.

KEYWORDS: *photosensitizer, cloth mask, personal protective equipment, reactive oxygen species, electrostatic interaction, COVID-19*

1. INTRODUCTION

Infectious diseases have always been severe threats to human health and safety globally, and the pandemic of COVID-19 in 2019−2020 has become a once per decade human crisis in many countries.[1,2] By August 26, 2020, the COVID-19 pandemic has caused over 23 million confirmed cases and more than 815 thousand death all over the world.[3] Since many respiratory infectious diseases are mainly transmitted via aerosol droplets, the application of personal protective equipment (PPE) such as face masks, protective suits, and face shields has shown effective roles in lowering the spread of the diseases.[4−6] However, PPE that is widely used can only physically block or electrostatically repel the pathogens with a limited lifetime, usually within several hours. Any live infectious pathogens surviving on the surface of the contaminated PPE could still cause cross-contamination during its reuse and disposal. However, sterilization and reuse of the current PPE have been an emergency practice during the COVID-19 pandemic due to the global shortage of PPE supplies.[7] Alternatively, cloth masks are recommended and affirmed as a tool to lower the virus transmittance in public.[8] Different cloth materials provide significant filtration efficiency against nanoscale aerosol particles,[9,10] yet surface-contaminated cloth face masks can still be a hazard and potentially contagious. Thus, the pathogen inactivation function of cloth masks has been proposed to inherently reduce cross-contamination during application and improve protection for the public.

Antimicrobial agents can be incorporated onto PPE materials to provide offensive protection by disinfecting and deactivating the pathogens. For instance, rechargeable *N*-halamine biocidal materials have been designed and intensively studied for food packaging, self-cleaning textiles, and water disinfection.[11−13] However, the release of free chlorine from *N*-halamine materials is a health concern when they are used in face masks. Moreover, a plasmonic heating effect of silver nanoparticle coating was successfully applied on N95 masks, achieving improved antimicrobial functions under light illumination, accompanied by an instant temperature increase

Received: August 28, 2020
Accepted: October 9, 2020
Published: October 22, 2020

https://dx.doi.org/10.1021/acsami.0c15540
ACS Appl. Mater. Interfaces 2020, 12, 49442−49451

to around 80 °C on the surface of the masks.[14] Although the high temperature could assist the biocidal property of the mask, it also poses concerns during the practical use in contact with the mouth and skin. On the other hand, photosensitizers could generate biocidal reactive oxygen species (ROS) in polymers under light exposure,[15] and the ROS could damage protein, DNA, and lipid of microorganisms to result in rapid inactivation. Benzophenone, anthraquinone, and xanthene derivatives are representative photoactive compounds and have been applied to polymers and fabrics to provide rapid antibacterial functions with acceptable washability and photostability.[16−18] Moreover, benzophenone structures were modified on the poly(vinyl alcohol-co-ethylene) nanofibrous membrane, achieving daylight-induced bioprotection with excellent bacterial and virus disinfection (i.e., 5−6 logs reduction) under light or even dark conditions.[15]

Herein, we present a new technology of fabricating photoinduced antibacterial and antiviral cotton fabrics (PIFs) through a simple chemisorption process, which is promising for industrial and mass production. Polycationic short chains were covalently formed by a nucleophilic substitution reaction and self-propagation of 2-diethylaminoethyl chloride (DEAE-Cl) on cotton fibers.[19] The resultant cationic cotton cloth is denoted as polyDEAE@cotton. The presence of the polycationic short chains on the cotton fibers makes them unique for the incorporation of light-induced antibacterial and antiviral anionic photosensitizers by chemisorption. Rose Bengal and anthraquinone-2-sulfonic acid sodium salt monohydrate (2-AQS) were employed as anionic photosensitizer (PS) examples to illustrate the affinity between polyDEAE@cotton and PSs and the bioprotective functions of the PIFs against bacteria and viruses. A cotton cationization agent was used to prove the proposed chemistry and uniqueness of the polyDEAE@cotton. The development of PIFs is expected to provide offensive protection as face masks and protective suits against pathogen-containing droplets to lower the spread and infection of COVID-19 as well as other infectious diseases.

2. MATERIALS AND METHODS

2.1. Chemicals. Plain cotton fabrics Style 400 (weighting 98 g/m^2, 60 × 60) was purchased from TestFabrics Inc. (West Pittston, PA, USA). DEAE-Cl, rose Bengal (RB) sodium salt (dye content ∼60%), 2-AQS, and L-histidine were bought from Sigma-Aldrich (St. Louis, MO, USA). (2-Chloro-2-hydroxypropyl)-trimethylammonium chloride (CHPTAC) was purchased from TCI (Portland, OR, USA). N,N′-Dimethyl-4-nitrosoaniline (*p*-NDA) was bought from Spectrum Chemicals & Laboratory Products (Gardena, CA, USA). All the chemicals were used as received without further purifications.

2.2. Cotton Modification with DEAE-Cl and CHPTAC. Cotton fabrics were activated in NaOH solution (120 g/L) at room temperature for 40 min. The liquor ratio was controlled at 1:50. The specific concentration of DEAE-Cl was prepared in isopropanol (IPA) (liquor ratio = 1:50). The activated cotton fabrics were removed from the NaOH system and transferred into the DEAE-Cl/IPA solution. The modification reaction is performed at 60 °C for 60 min. Then, the DEAE-Cl modified cotton fabrics (polyDEAE@cotton) were washed with an excess amount of deionized water and dried at 80 °C for 5 min.

The modification of the cotton fabric by CHPTAC was performed by treating the fabric in 50 g/L NaOH solution at room temperature for 30 min. Then, CHPTAC was added to reach a final concentration of 30 g/L. The mixture was further reacted at 80 °C for 60 min. The resultant fabric, denoted as CHPTAC@cotton, was washed with deionized water and dried at 80 °C for 5 min.

2.3. Functionalization of PolyDEAE@cotton with PSs. Two anionic PSs, RB and 2-AQS, were selected to functionalize polyDEAE@cotton for achieving daylight-induced antibacterial/antiviral functions as a PIF, which was easily performed under traditional dyeing process. PS solutions were prepared by dissolving a specific amount of RB or 2-AQS in deionized water and were used as dyeing solutions. A fabric to PS solution ratio (liquor ratio) was controlled at 1:50. The solution pH was adjusted to 6.0 with 0.1 M HCl solution. For RB dyeing, first, the polyDEAE@cotton or pristine cotton was wetted with water and squeezed before putting into a dyeing bath (60 °C) for 10 min. Afterward, the temperature of the dyeing bath was increased to 90 °C within 10 min, and the RB dyeing was further continued for 30 min at 90 °C. On the other hand, the dyeing of 2-AQS was accomplished at 60 °C for 40 min. Then, the dyed fabrics were washed thoroughly with soap water and cold water and dried at 80 °C for 5 min. The adsorption amounts of PSs on the fabrics were measured based on the PS concentration changes after dyeing. The calibration curves for quantify the concentrations of RB (C_{RB}) and 2-AQS ($C_{2\text{-}AQS}$) in mg/L are $A_{550} = 0.0093 \times C_{RB}\text{-}0.0322$ ($R^2 = 0.9935$) and $A_{330} = 0.016 \times C_{2\text{-}AQS} + 0.012$ ($R^2 = 1.0000$), respectively.

2.4. Characterizations. Scanning electron microscope (SEM) images were captured using a FE-SEM (Quattra ESEM, Thermo Fisher Scientific, USA). Thermogravimetric analysis (TGA) was performed with a TGA-60 system (Shimadzu Science Instruments, Inc., USA). The sample weight was around 10 mg. First, the sample was heated from room temperature to 120 °C (rate = 20 °C/min) and held for 3 min to eliminate free water with N_2 flow (30 mL/min). Then, the sample was cooled to room temperature with the protection of an N_2 atmosphere and reheated to 600 °C (rate = 10 °C/min).

The presence of polycationic short chains on the cellulose surface was proved and evaluated by an indirect method: adsorption of negatively charged protein of bovine serum albumin (BSA). In detail, around 200 mg of PIF was immersed in 1 g/L BSA solution (pH = 7.4) and stored at 4 °C for 24 h. The BSA concentration before and after fabric adsorption was quantified with bicinchoninic acid (BCA) protein assay. The testing solution was prepared by mixing 2 mL of BCA reagent A, 40 μL of BCA reagent B, and 100 μL of sample solution. The mixture was incubated at 37 °C for 30 min; then, the color intensity of the mixture was monitored using a UV−vis spectrophotometer. The BSA concentration in g/L (C_{BSA}) was calculated based on the absorbance intensity at a wavelength of 560 nm (A_{560}) according to an established calibration curve of $C_{BSA} = 1.2171 \times A_{560}\text{−}0.1355$, $R^2 = 0.9957$. The water contact angle of the fabrics was measured using a Dino-Lite microscope (Dunwell Tech. Inc., USA) by dropping 10 μL of distilled water on the fabric; the images at a specific time interval after water-dropping were captured with DinoCapture 2.0.

2.5. Measurement of ROS. Here, *p*-NDA was selected as a highly selective hydroxyl radical scavenger for ROS measurements.[20,21] The PIF (2 cm × 2 cm) was immersed in 10 mL of 40 μM *p*-NDA solution in a glass Petri dish. Then, the samples were exposed to daylight in an XL-1500 crosslinker for 30 min. The light intensity in the crosslinker was measured using a light meter (EXTECH, Model # LT300) to be 13000 Lux. As a reference, the light intensity of outdoor under the sun (on July 22, 2020, in Davis, CA, USA), outdoor in the shade (on July 22, 2020, in Davis, CA, USA), in office, and in a supermarket was measured to be 87,000, 3000, 1000, and 600 Lux, respectively. The color fading of the *p*-NDA solution, contributed to the quenching by hydroxyl radicals produced from the PIF, was detected with a UV−vis spectrophotometer. The concentrations of *p*-NDA solution in 1×10^{-5} M ($C_{p\text{-}NDA}$) before and after light illumination were calculated according to a calibration curve ($A_{440} = 0.3387 \times C_{p\text{-}NDA}\text{-}0.0095$, $R^2 = 0.9998$), and the maximum absorption intensity at a wavelength of 440 nm (A_{440}) was recorded. The concentration change of the *p*-NDA ($\Delta C_{p\text{-}NDA1}$) was applied to evaluate the production of hydroxyl radicals by PIFs. For testing the generation of singlet oxygen from PIFs, 0.01 M L-histidine was added into the *p*-NDA solution.[21] In this case, the decrease of the *p*-NDA

https://dx.doi.org/10.1021/acsami.0c15540
ACS Appl. Mater. Interfaces 2020, 12, 49442−49451

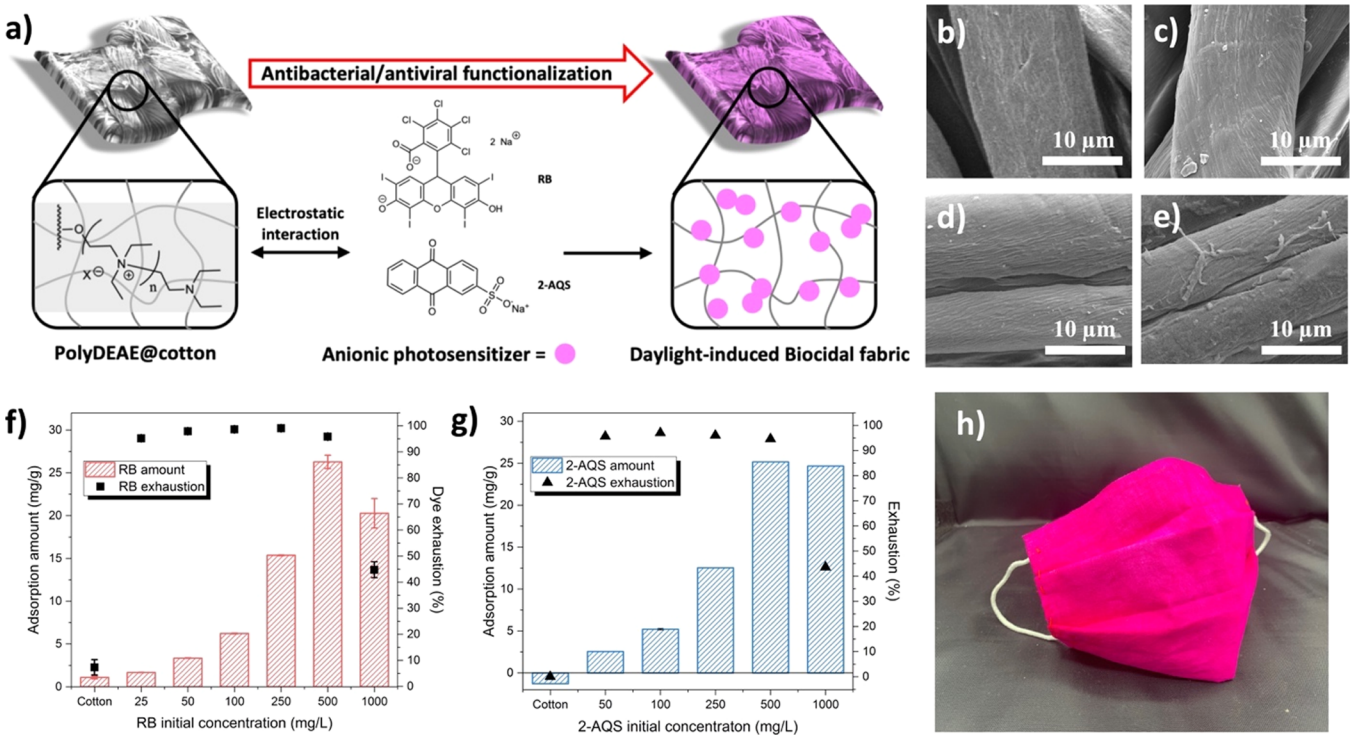

Figure 1. (a) Schematic illustration of the fabrication of daylight-induced antibacterial and antiviral textiles. SEM images of (b) cotton, (c) polyDEAE@cotton, and (d) RB-dyed polyDEAE@cotton. (e) 2-AQS-dyed polyDEAE@cotton. Adsorption amount and dye exhaustion of (f) RB and (g) 2-AQS on polyDEAE@cotton with different initial concentrations. The "cotton" in the *x* axis means pristine cotton dyed with 250 mg/L RB or 2-AQS. (h) Design of a face mask based on PIFs.

concentration ($\Delta C_{p\text{-NDA2}}$) was attributed to the quenching of *p*-NDA by hydroxyl radicals and the singlet oxygen oxidized L-histidine. The production of singlet oxygen by PIFs under daylight illumination can be evaluated by the difference between $\Delta C_{p\text{-NDA1}}$ and $\Delta C_{p\text{-NDA2}}$. It is important to note that there is no color fading of *p*-NDA solution either under a dark condition or under light but without PIFs (Figure S1).

2.6. Antibacterial Test. The antibacterial function of PIFs was examined against two model bacteria: gram-negative *Escherichia coli* O157:H7 [American Type Culture Collection 700,728] and gram-positive *Listeria innocua* [American Type Culture Collection 33090]. The bacterial culture was processed by mixing *E. coli* and *L. innocua* colonies with 10 mL of lysogeny broth and 10 mL of trypticase soy broth, respectively, and incubated at 37 °C for 24 h. Thereafter, around 4×10^6 CFU mL^{-1} *E. coli* and 1×10^5 *L. innocua* cultures can be obtained for further antibacterial tests.

Before the antibacterial test, the bacterial culture solution was subjected to 2 cycles of centrifugation (5000 rpm, 8 min) and washing (10 mL of cold phosphate-buffered saline) processes. Then, 20 mL of phosphate-buffered saline (PBS) was mixed with the bacterial precipitate as the final bacterial culture suspension. PIFs (2 cm × 2 cm) were placed in a Petri dish and wet with 20 μL of bacterial culture suspension. Here, 0.1 wt % Triton X-405 was added in the bacterial culture solution to assist the complete wetting of hydrophobic samples. Then, different fabrics were exposed to daylight in an XL-1500 crosslinker or incubated under the dark condition for different durations. Sterile PBS (20 μL) was dropped on the sample surface every 5 min to avoid the killing effect from elevated temperature during light illumination. After this, the residual bacteria on the fabric were extracted with 1 mL of sterile PBS buffer and were serially diluted ($\times 10^0$, $\times 10^1$, $\times 10^3$, $\times 10^5$) to be inoculated on a lysogeny agar plate (*E. coli*) or trypticase soy agar plate (*L. innocua*) for bacterial enumeration at 37 °C for 24 h. The quantification of antibacterial function was evaluated by the plate count of residual bacterial CFU numbers. All the bacterial reduction was calculated based on the CFU number obtained on the pristine cotton, and it showed negligible effects on the killing of bacteria.

2.7. Antivirus Test against T7 Bacteriophage. T7 bacteriophage was selected as a model viral target in this study based on the results of our previous study in which we demonstrated that photoinactivation resistance of T7 was relatively higher/similar compared to a model coronavirus.[22] T7 bacteriophage was prepared according to a procedure provided in the Supporting Information. 1×10^7 PFU mL^{-1} T7 bacteriophage suspension (10 μL) was uniformly loaded on the surface of PIFs or control samples in a size of 2×2 cm^2. The samples were then placed under dark conditions or daylight irradiation for different durations. At each specific time point, the samples were vortexed vigorously with 3 mL of maximum recovery diluent to collect the T7 phages from the fabrics. After serial dilution, 100 μL of the phage dilution was mixed with 200 μL of *E. coli* BL21 (1×10^9 CFU mL^{-1}) suspension and incubated for 10 min at 37 °C. Molten Luria Bertani (LB) agar (3 mL) at 45 °C was then mixed with the T7 phage-*E. coli* mixture followed by immediately pouring onto a prewarmed LB agar plate. After agar solidification, the plates were incubated overnight at room temperature, after which the phage plaques were counted and standardized to the initial concentration.

2.8. Light and Washability Tests. The as-fabricated PIFs were exposed to office light for 7 days. The light intensity was measured using a light meter (EXTECH, Model # LT300) to be around 1000 Lux. According to AATCC Test Method 107−2009 and AATCC Test Method 61−1996, the washability of the fabrics was performed in a beaker (1st wash) and with a Launder-O-Meter (2nd and 3rd washes). For the first-time wash, PIFs were immersed in 300 mL of deionized water with 0.3 wt % detergent. The mixture was stirred (200 rmp) for 45 min at 40 °C. Then, the fabrics were rinsed with deionized water to remove the detergent and dried at 80 °C for 3 min. By using the Launder-O-Meter, PIFs (2×6 in^2) were immersed in 150 mL of water containing 0.225 g detergent with 50 steel balls. Then, the washing was performed in the Launder-O-Meter at 50 °C for 45 min. Afterward, the PIFs were rinsed with water and dried at 80 °C for 3 min. The bioprotective functions of the PIFs were evaluated

https://dx.doi.org/10.1021/acsami.0c15540
ACS Appl. Mater. Interfaces 2020, 12, 49442−49451

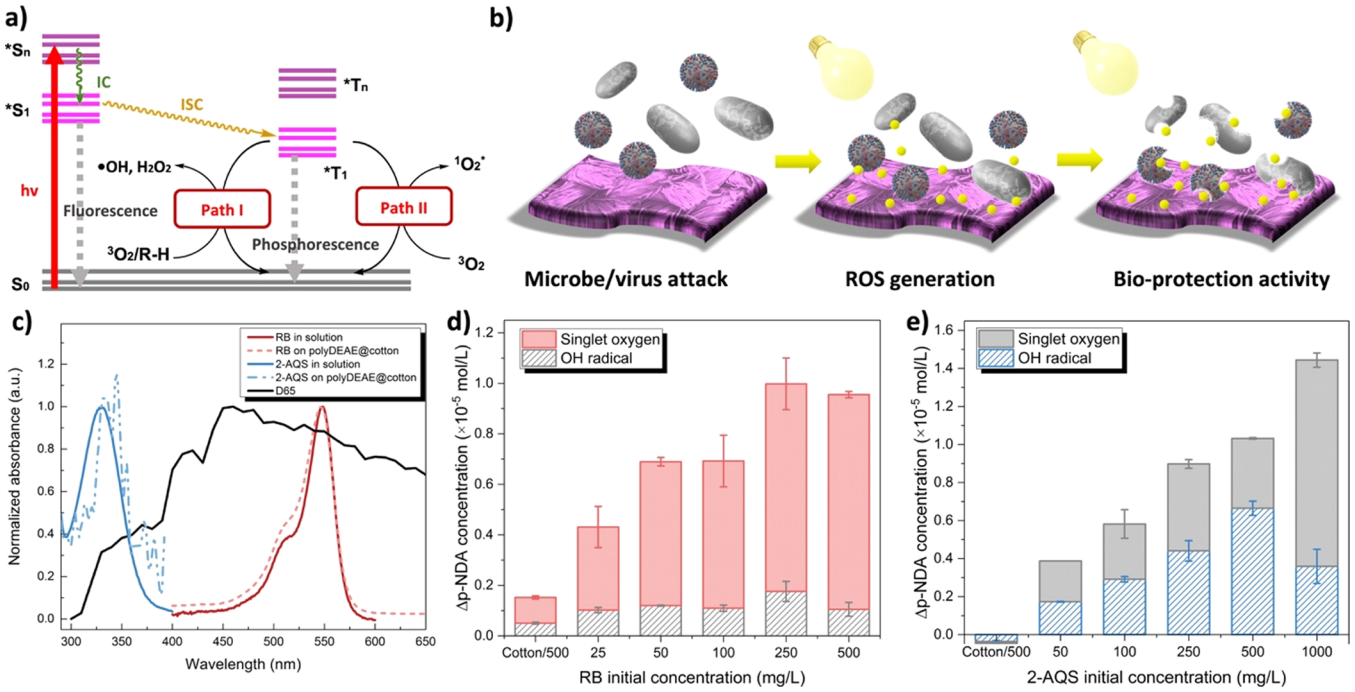

Figure 2. (a) Jablonski diagrams illustrating the daylight excitation of a photosensitizer to the singlet state and following intersystem crossing to the triplet state, finally performing the generation of ROS via path I and path II mechanisms. (b) Scheme of the daylight-induced functions of PIFs. (c) Normalized UV−vis spectra of RB and 2-AQS aqueous solutions and adsorbed on the polyDEAE@cotton accompanied by the spectrum of the D65 standard light source. Measurement of ROS production from (d) RB-polyDEAE@cotton and (e) 2-AQS-polyDEAE@cotton according to RB and 2-AQS initial concentrations under 30 min daylight illumination. The "Cotton/500" in the *x* axis refers to the pristine cotton dyed with 500 mg/L RB and 500 mg/L 2-AQS solution, respectively.

through antibacterial tests. Each time of the washing in the Launder-O-Meter is equivalent to 5 times of household handwashing.

3. RESULTS AND DISCUSSION

3.1. Preparation of PIFs. The design of PIFs was guided by three criteria: (i) the PIFs can be easily fabricated with industrial scalability; (ii) the fabrics must show efficient antibacterial and antiviral functions under daylight illumination; and (iii) the fabrics must provide good surface contact to pathogens to ensure the efficient contact-kill. In order to achieve the first requirement, cotton fabric was selected as the substrate with the advantages of being naturally derived, widely used in cloth face masks, and environmentally friendly. The last two criteria were satisfied by uniquely incorporating polycationic structures onto cotton fiber surfaces to provide strong electrostatic interactions with anionic PSs. The antibacterial and antiviral functions resulted from the efficient production of ROS by the electrostatically incorporated PSs under light illumination. Here, two known anionic PSs, 2-AQS and RB, were selected as representatives, which could generate ROS through different paths under light illumination.[23−25] On the other hand, an innovative modification of cotton with DEAE-Cl achieved the growth of polycationic short chains on the cotton fibers. The presence of the polycationic short chains (denoted as polyDEAE) on the cotton fibers not only provides the electrostatic interactions for PS functionalization but also assists the affinity of PIFs to negatively charged bacteria (e.g., *E. coli* and *L. innocua*) and viruses (e.g., enveloped coronavirus), which is crucial for the biocidal efficiency of the PIFs. The modification of cotton cellulose with polyDEAE was achieved via a two-step reaction, including cotton activation with 120 g/L NaOH solution and polyDEAE growth based on nucleophilic substitution and self-propagation of DEAE-Cl (Scheme S1). Then, the functionalization of polyDEAE@cotton with PSs through electrostatic chemisorption is illustrated in Figure 1a. The surface morphology of the cotton after different treatments was examined under the SEM (Figure 1b−e). There is no obvious surface morphology change of the cotton fibers after polyDEAE growth, indicating that the size of the polyDEAE short chains was at the molecular level. Similarly, no significant morphology change of the cotton fibers was noticed under the SEM after PS functionalization. In spite of this, the chemical structures and component variations of the PIFs were confirmed through FTIR and TGA (Figure S2).

The antibacterial and antiviral functions of PIFs are provided by the incorporated anionic PSs on the polyDEAE@cotton, a result of strong electrostatic interactions between two ionic groups with opposite charges.[19] Different initial concentrations of RB and 2-AQS were applied to examine the attractive static interactions with the polycationic short chains on the polyDEAE@cotton. As shown in Figure 1f, the RB adsorbed on the polyDEAE@cotton increased, as the initial concentration of RB was increased from 25 to 500 mg/L, and became steady if the RB concentration was further increased to 1000 mg/L. From the calculated dye exhaustion by the fabrics in Figure 1f, more than 95% of the RB in solution (initial concentration ranging from 25 to 500 mg/L) was attracted onto the polyDEAE@cotton after the 40 min dyeing process, whereas the dye exhaustion rate dropped to around 45.0% when the RB concentration reached 1000 mg/L. A similar phenomenon can be noticed for the use of 2-AQS as a PS, as presented in Figure 1g. The 2-AQS exhaustions by the polyDEAE@cotton were tested to be >95%, when the initial 2-

https://dx.doi.org/10.1021/acsami.0c15540
ACS Appl. Mater. Interfaces 2020, 12, 49442−49451

Table 1. Surface Hydrophobicity and Daylight-Induced Antibacterial Function of PS-Adsorbed polyDEAE@Cotton Fabrics

samples	WCA (°) (1 s/20 s)	the reduction rate of bacterial count (%)			
		E. coli (10^6 CFU/mL)		*L. innocua* (10^5 CFU/mL)	
		30 min	60 min	30 min	60 min
Pristine cotton	0/0	0.00%	0.00%	0.00%	0.00%
polyDEAE@cotton	0/0	98.50%	99.25%	85.75%	96.19%
50 mg/L RB	108.2/0	99.99%	99.9999%	99.999%	99.999%
100 mg/L RB	114.2/0	77.50%	99.99%	99.999%	99.999%
250 mg/L RB	122.0/120.0	6.07%	99.29%	99.98%	99.999%
250 mg/L AQS	85.0/0	99.97%	99.9999%	99.98%	99.98%
500 mg/L AQS	110.0/0	99.9999%	99.9999%	99.999%	99.999%

AQS concentration was below or at 500 mg/L, and then dropped to 43.6% when the concentration reached 1000 mg/L, due to saturation of adsorption of the anionic molecule. More importantly, the presence of polycationic short chains on the polyDEAE@cotton is crucial for ensuring the biocidal functions by having sufficient amounts of PSs on the PIFs. The highest adsorption amounts of both RB and 2-AQS on the polyDEAE@cotton were found at 26.28 mg/g and 25.16 mg/g, respectively. In contrast, the pristine cotton only showcased 1.09 mg/g of RB adsorption and no affinity to 2-AQS at the PS initial concentration of 500 mg/L (Figure 1f,g). The optical images of the PIFs and a demo of using PIFs for face mask design are shown in Figure S3 and Figure 1h, respectively. The growth of the polyDEAE on the cotton fibers leads to high exhaustion of PSs by the polyDEAE@cotton, making the fabrication of PIFs efficient, green, and environmentally friendly by reducing residual PSs in the wastewater.

3.2. Photoactivity of PIFs under Daylight Illumination. The generation of ROS on the PIFs under daylight represents desired biocidal functions against both bacteria and viruses.[25] The specific mechanism of ROS generation from PSs under light can be explained by the Jablonski diagram illustrated in Figure 2a. The achievement of the triplet excited state ($^*T_n$) of the PS through intersystem crossing is essential for generating ROS, including hydroxyl radicals (•OH), superoxide radicals ($\bullet O^{2-}$), hydrogen peroxide (H_2O_2), and singlet oxygen ($^1O_2$), in the presence of oxygen, which consequently performs biocidal functions. The generated ROS are strong oxidants, which can damage DNA, RNA, proteins, and lipids of microorganisms, contributing to the antibacterial and antiviral functions.[26,27] Figure 2b showcases the diagrammatic illustration of biocidal functions of the PIFs under daylight exposure. Once the pathogens are attached on the surface of the PIFs, the light-induced ROS could instantly kill the bacteria or viruses.

To gain an insight into the photoexcitation process of PSs on PIFs, we used time-dependent density functional theory (TD-DFT) calculations to evaluate the photoactivity of RB and 2-AQS. The required energy for triggering the excitation from the ground state of the PS to its singlet excited state can be visually examined through the UV−vis absorption spectrum of the PS. As shown in Figure 2c, the maximum absorption wavelength (λ_{max}) of 2-AQS and RB appears at 330 and 550 nm, respectively. Given that the light absorption of RB completely lies in the visible range, the ROS production from the RB excitation under daylight is expected to be efficient. Although the λ_{max} of 2-AQS showcases in the UV range, the light energy provided by a D65 standard light source ranging from 300 to 400 nm can still trigger the photoexcitation (Figure 2c).

The presence of anionic carboxylate in RB and sulfonate groups in 2-AQS structures makes them attractive to the polycationic short chains on the polyDEAE@cotton, leading to an easy functionalization of cotton cloth with photo-induced antibacterial and antiviral properties. Nevertheless, it is essential to investigate the photoactivity of PSs after the formation of the electrostatic pairs with polyDEAE@cotton. As presented in Figure 2c, the λ_{max} of RB and 2-AQS on the polyDEAE@cotton shows a negligible difference to that of the PS in aqueous solution, illustrating no influence on the energy requirement of photoexcitation. Meanwhile, according to TD-DFT calculation of RB and 2-AQS, neither the carboxylate nor the sulfonate orbital involved in the achievement of excited singlet and triplet states of the PSs (Figure S4). Since the photoactivity of RB and 2-AQS is excluded from their anionic groups, the adsorption of RB and 2-AQS on the polyDEAE@cotton based on electrostatic interaction would not disturb their photoexcitation process. Meanwhile, the RB- and 2-AQS-dyed PIFs showed similar absorption spectra to the free PSs (Figure 2c), making the photoexcitation of PIFs identical to that of the PS in the water system.

To evaluate the photoactivity of PIFs, the production of ROS by both RB- or 2-AQS-dyed polyDEAE@cotton, denoted as RB-polyDEAE@cotton or 2-AQS-polyDEAE@cotton, was examined with daylight illumination for 30 min (Figure 2d,e). Consistent with other studies, RB is a good producer of singlet oxygen ($^1O_2$) via the path II photoreaction mechanism with a negligible amount of •OH production. By increasing the initial concentrations of RB in the dyeing solution, the RB-polyDEAE@cotton produced more $^1O_2$, which is super oxidative but short-lived. Nevertheless, only around 0.1×10^{-5} mol/L *p*-NDA was bleached by •OH, a ROS produced as a result of photoreaction path I, indicating that RB molecules in the RB-polyDEAE@cotton still exclusively undergo the path II photoreaction. Alternatively, anthraquinones are a group of PSs performing both path I and path II mechanisms of ROS production. As presented in Figure 2e, the amounts of generated •OH and $^1O_2$ on the 2-AQS-polyDEAE@cotton samples were comparable except for the one dyed with 1000 mg/L 2-AQS. The total generation of ROS (e.g., •OH and $^1O_2$) was increased with more 2-AQS incorporating on the surface of the polyDEAE@cotton, a piece of evidence that the self-quenching of the ROS on the fabrics was not severe in the tested concentration range of 2-AQS. A high concentration of 2-AQS on the surfaces of the fibers may block its access to the hydrogen donor in the path I reaction (R−H in Figure 2a), without affecting the path II reaction, and consequently reduce the generation of •OH. However, the adsorption amount of RB, as well as the $^1O_2$ production, on the RB-polyDEAE@

https://dx.doi.org/10.1021/acsami.0c15540
ACS Appl. Mater. Interfaces 2020, 12, 49442−49451

cotton reached saturation when the initial dyeing concentration of RB was 1000 mg/L.

As a summary, by taking the merit of the strong electrostatic interaction between the polyDEAE cationic short chains on the cotton fibers and the anionic PSs, the photoactivity of PSs was successfully retained on the substrate, allowing the resultant PIFs as potential biocidal functional materials for applications in PPE like cloth masks and protective suits against pathogen attack.

3.3. Antibacterial Functions of PIFs. To obtain an insight on the biocidal function of the PIFs, RB-polyDEAE@cotton and 2-AQS-polyDEAE@cotton were challenged by direct contact with bacteria. The PIFs were inoculated with *E. coli* (Gram-negative) and *L. innocua* (Gram-positive) suspensions individually and then exposed to daylight illumination for 30 or 60 min. The bacterial reduction rates on the PIFs were determined by comparing the ratios of colony counts from different PIFs and pristine cotton samples (Table 1). The pristine cotton presents no biocidal functions, while the quaternary ammonium salts on the polyDEAE@cotton lead to rather limited antibacterial performance under both light and dark conditions (reduction around 1−2 logs). Without light exposures, however, the biocidal functions of PS-dyed PIFs were decreased and finally eliminated with increasing amounts of anionic PSs on the fabrics (Table S1). Therefore, the bacterial reduction on the PIFs under the daylight illumination is solely attributed to the photo-induced ROS oxidations. Residual excess cationic polyDEAE sites should still exist on the PIFs but did not show noticeable biocidal outcomes. However, their affinity to the anionic microorganism is expected to facilitate the antibacterial and antiviral functions of the PIFs.

As summarized in Table 1, both *E. coli* and *L. innocua* appeared to be susceptible to the PIFs under light illumination. Interestingly, with increasing the initial RB concentration from 50 to 250 mg/L, the biocidal function of the PIFs dropped dramatically from 6 log reduction to only 2 log reduction under 60 min daylight exposure. This phenomenon was more obvious when the light illumination was shortened to 30 min (Table 1). The hydrophobicity of the RB-polyDEAE@cotton increased by having more hydrophobic RB aggregated on the surface, reducing contact of the surface with microorganisms, and potentially lowering the biocidal function of the PIFs. However, this issue was not observed in 2-AQS-dyed PIFs, and its killing efficiency toward both *E. coli* and *L. innocua* can be improved by increasing the amount of 2-AQS on the fabrics (Table 1). Here, the surface properties of the PIFs modified by different concentrations of RB and 2-AQS were examined by measuring their water contact angles (WCAs) (Table 1). The hydrophobicity increase of the PIFs would reduce surface contact and lower the reduction against bacteria. For RB-dyed PIFs, the initial concentration of RB at 50 mg/L (i.e., 3.35 mg/g RB on the PIFs) achieved the best killing performance against both *E. coli* and *L. innocua* and exhibited bacterial reduction rates of 99.99 and 99.9999% with 30 and 60 min daylight exposure, respectively. The PIFs dyed with 2-AQS also showcased effective biocidal functions with 5−6 logs of reductions against both gram-positive and gram-negative bacteria after 60 min light exposure (Table 1).

3.4. Bioprotective Function Expansion to Other Cationic Cotton Cloth. The use of electrostatic interaction to functionalize polyDEAE@cotton with PSs opens a new approach to produce novel functional textiles, and consequently, the cationic cotton could serve as a platform. With such a hypothesis, cotton fabrics modified with other cationic moieties can also be applied as the substrate. For instance, CHPTAC was developed to treat cotton fabrics for salt-free reactive dyeing and could be a potential alternative.[28] The cotton fabrics were modified with CHPTAC (CHPTAC@cotton) according to a reaction shown in Scheme S2, and the treated cotton was employed to adsorb RB and 2-AQS. At the initial concentrations of RB (100 mg/L) and 2-AQS (250 mg/L), the adsorption amounts of both agents on the CHPTAC@cotton were 5.719 mg/g (RB) and 12.346 mg/g (2-AQS), respectively, which are comparable to those adsorbed on the polyDEAE@cotton. As summarized in Table 2, the resultant PIFs showed efficient antibacterial functions against both *E.coli* and *L. innocua*, with reduction rates examined around 2−6 logs under 60 min daylight illumination.

Table 2. Daylight-Induced Antibacterial Function of PS-Adsorbed CHPTAC@Cotton Fabrics

samples	the reduction rate of bacterial count (%)	
	E. coli (10^6 CFU/mL)	*L. innocua* (10^5 CFU/mL)
	60 min	60 min
Pristine cotton	0.00%	0.00%
CHPTAC@cotton	99.52%	50.00%
100 mg/L RB	99.98%	99.999%
250 mg/L AQS	99.9999%	99.97%

Interestingly, the presence of excessive polyDEAE cationic sites on the fabric could provide strong interactions toward anionic cell membranes of microorganisms, improving the biocidal efficiency of the PIFs due to the improved surface contacts.[29,30] As a proof of this hypothesis, an anionic protein of BSA was selected as a microorganism mimic to evaluate the affinity between the PIFs and pathogenic microorganisms. As shown in Figure 3a, once the initial dyeing concentration of RB reached 250 mg/L, the cationic sites on the RB-polyDEAE@cotton became almost fully covered, and the fabric lost its affinity toward negatively charged BSA. Similarly, almost all cationic sites on the 2-AQS-polyDEAE@cotton were consumed by 2-AQS when its initial dyeing concentration reached 1000 mg/L, and the fabric showed a negligible affinity to extra anionic proteins (Figure 3b). On the other hand, the adsorption affinities between the CHPTAC@cotton, RB-CHPTAC@cotton, 2-AQS-CHPTAC@cotton, and BSA were very weak, presenting almost no protein adsorption in Figure 3c. This fact can be explained as the relatively weak attractive force of single cationic sites on the CHPTAC@cotton toward large molecules of anionic proteins, and this phenomenon was reported in the literature.[31] In this case, the existence of the polyDEAE cationic short chains on the cotton ensures the sufficient adsorption of anionic PSs on the surface and provides additional attractions to anionic microorganisms.

Consequently, with comparable amounts of PS adsorbed on both polyDEAE@cotton and CHPTAC@cotton, the lack of extra interaction toward microorganisms of the CHPTAC@cotton resulted in less efficient biocidal functions. Upon 60 min daylight irradiation, the reduction rates of *E. coli* and *L. innocua* by RB-CHPTAC@cotton were about 2 logs lower than those of the RB-polyDEAE@cotton (Tables 1 and 2). Nevertheless, the biocidal efficiency difference was blurred when 2-AQS was employed on the PIFs since •OH is a

https://dx.doi.org/10.1021/acsami.0c15540
ACS Appl. Mater. Interfaces 2020, 12, 49442−49451

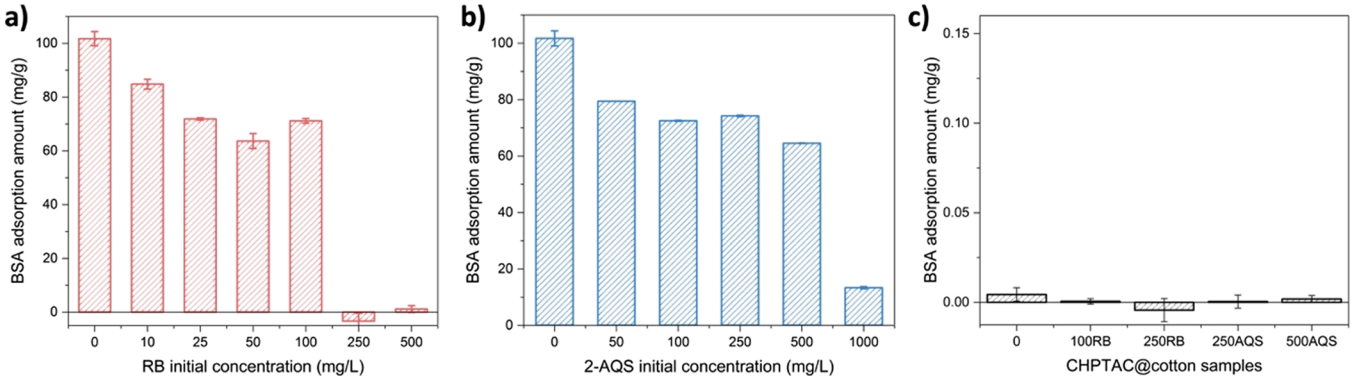

Figure 3. Adsorption of negatively charged protein (BSA) on (a) RB-polyDEAE@cotton, (b) 2-AQS-polyDEAE@cotton, and (c) CHPTAC@cotton dyed with different initial concentrations of RB and 2-AQS.

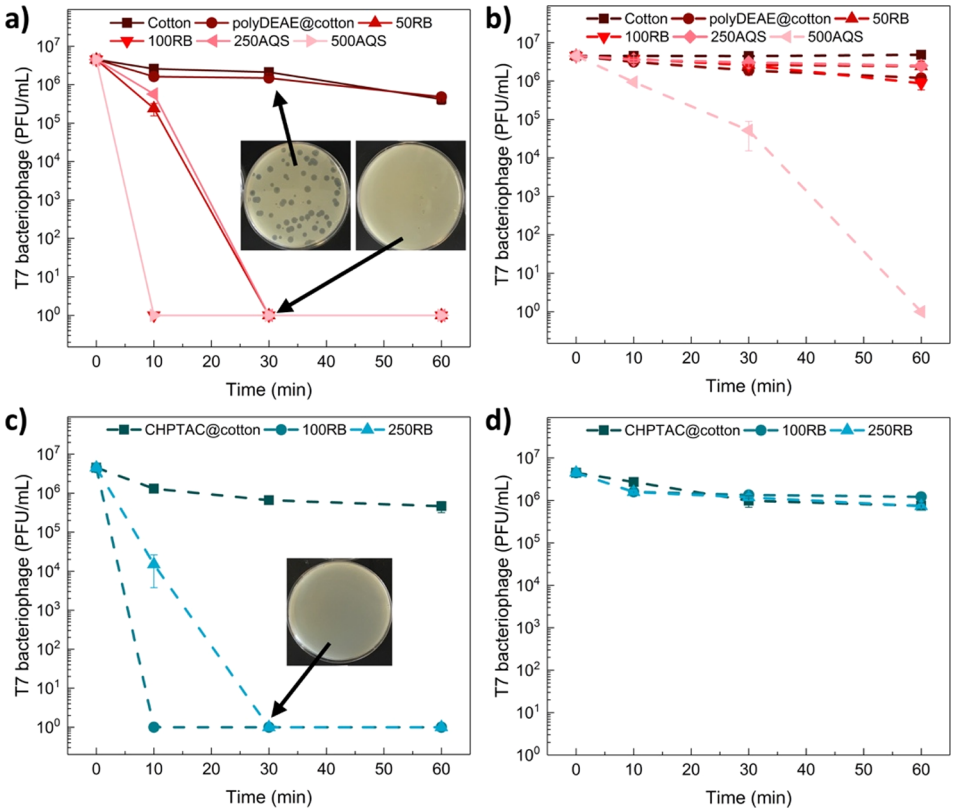

Figure 4. Antiviral results of polyDEAE@cotton-based PIFs (a) with daylight illumination and (b) under dark condition. Antiviral results of CHPTAC@cotton-based PIFs (c) with daylight illumination and (d) under dark condition. The inserted photo in (a) illustrates the virus count on pristine cotton (left) and PIFs (right) after 30 min daylight illumination, and (c) virus count on CHPTAC@cotton-based PIF after 30 min daylight illumination.

reactive and less selective oxidant than $^1O_2$,[32] which can be generated by 2-AQS under light illumination. Overall, the CHPTAC@cotton still can serve as a good intermedium for effectively incorporating reactive species to provide desired photoactive functions.

3.5. Antiviral Functions of PIFs. The generation of strong oxidants of ROSs by PIFs under daylight makes the biocidal function nonselective and applicable for a broad-spectrum of biological applications. Due to the fact that we were unable to test the biocidal function of PIFs against SARS-CoV-2, to get an insight on the bioprotective function of PIFs against viruses, T7 bacteriophage was selected as a surrogate of mammalian viruses to inoculate onto the PIFs under daylight illumination, since early results indicated that T7 bacteriophage was more resistant to ROS than some coronavirus.[22] Cotton and polyDEAE@cotton showed no obvious biocidal functions against T7 bacteriophage either with light exposure or under dark conditions (Figure 4a,b). On the contrary, the PIFs containing different amounts of RB or 2-AQS present rapid and efficient killing of T7 bacteriophage, resulting in more than 6 log reduction of plaque-forming units (PFU) with 30 min or longer contact under daylight exposures. It further proved that the antiviral function of the PIFs is highly attributed to the efficient generation of ROS by the PSs under daylight exposure. Excitingly, the complete kill of the T7 phage (6 logs PFU) can even be achieved in only 10 min of contact with PIFs dyed with higher concentrations of PSs, such as 100 mg/L RB and 500 mg/L 2-AQS, though there were 16.52 and

https://dx.doi.org/10.1021/acsami.0c15540
ACS Appl. Mater. Interfaces 2020, 12, 49442−49451

Table 3. Washability and Photostability of PS-Dyed polyDEAE@Cotton Fabrics in Terms of Antibacterial Functions (60 min Daylight Irradiation)

samples	the reduction rate of bacterial count (%)									
	E. coli (10^6 CFU/mL)					*L. innocua* (10^5 CFU/mL)				
	before wash	1st wash	2nd wash[a]	3rd wash[a]	after 7 days of light exposure	Before wash	1st wash	2nd wash[a]	3rd wash[a]	after 7 days of light exposure
50 mg/L RB	99.9999%	99.9997%	99.9999%	99.9999%	99.9999%	99.999%	99.98%	99.9999%	99.9999%	99.999%
100 mg/L RB	99.99%	99.9995%	99.99%	99.98%	99.9999%	99.999%	99.999%	99.999%	99.999%	99.999%
250 mg/L AQS	99.9999%	65.71%			99.74%	99.999%	99.94%			98.10%

[a]The wash was performed with Lander-O-Meter and each washing equals to 5 times of household hand washes.

79.13% of the virus PFU decreases on the PIF under the dark condition (Figure 4a,b). 2-AQS itself might be toxic to T7 bacteriophage, especially in high concentrations (Figure 4b).

Moreover, the PIFs modified on CHPTAC@cotton with 100 mg/L RB or 250 mg/L 2-AQS also showcased highly efficient killing effects against T7 bacteriophage (Figure 4c). Again, CHPTAC@cotton performed no biocidal functions regardless of light illumination. A 6 log reduction of T7 bacteriophage was achieved on RB-CHPTAC@cotton and 2-AQS-CHPTAC@cotton after 10 and 30 min of daylight exposure, respectively. Meanwhile, there were negligible decreases of bacteriophage PFU count on the PIFs under dark conditions (Figure 4d), which further demonstrated the essential role of ROS generated on the PIFs for ensuring the bioprotective function.

Here, the results proved the broad application potential of using cationic cotton as a platform for cotton fabric functionalization by anionic PSs as photo-induced biocidal agents. RB on polycationic cotton (RB-polyDEAE@cotton) seems an ideal combination.

3.6. Stability and Washability of PIFs. The washability and photostability of the PIFs are crucial for their long-term use in practical applications, and PIFs made from polyDEAE@cotton were selected. The first-time wash of the PIFs was performed in soap water at 40 °C for 45 min. As shown in Table 3, the PIFs retained their efficient antibacterial functions after the first washing. More interestingly, the PIF dyed in 100 mg/mL of RB presents an increased (1 log higher) bacterial reduction after the first wash, which could be caused by increased surface hydrophilicity. Although the washing with anionic surfactants could remove certain surface-adsorbed RB from the PIFs, the strong electrostatic interactions of polyDEAE cationic chains with RB molecules, as well as the hydrophobic nature of RB, slowed down the further removal of the photoactive agents from the fabrics. Meanwhile, there is no dye leaching from the PIFs when the fabrics were immersed in water without surfactants. To further prove the feature of the fabrics, a Launder-O-Meter washing procedure was applied to the PIFs dyed with 50 and 100 mg/L RB. According to AATCC Test Method 61−1996, each washing process is equivalent to 5 times of household hand wash.[33] The samples were additionally washed in a Launder-O-Meter for another two times, and then, the samples were challenged with both *E. coli* and *L. innocua* under 60 min daylight illumination. The PIFs successfully maintained their efficient biocidal functions against *E. coli* and *L. innocua*. Even after washing 2 times, equivalent to 10 times of hand washes, the RB-polyDEAE@cotton still exhibited 3−5 logs of bacterial reduction (Table 3). On the other hand, 2-AQS molecules on the 2-AQS-dyed PIFs were less tolerant to the washing process, possibly due to the high hydrophilicity. Antibacterial functions of the fabric dropped to only 65.71 and 99.94% reduction to *E. coli* and *L. innocua*, respectively (Table 3). In this regard, 2-AQS-dyed PIFs might not be ideal for long-term application and reuse, so no further Launder-O-Meter washing was performed on 2-AQS-dyed PIFs.

PSs will suffer from photobleaching under light illumination and gradually lose their functions during long-term usage even without any biological burdens. Therefore, the PIFs, including RB- and 2-AQS-dyed fabrics, were challenged by continuous daylight exposure for 7 days, and, then their retained antibacterial functions were examined. Again, the longtime daylight challenge can cause color fading of the PIFs, whereas the antibacterial function of the RB-dyed PIFs was retained. Nevertheless, a slight decrease of the biocidal functions of 2-AQS-dyed PIFs was noticed. The results are shown in Table 3.

Overall, the RB-dyed PIFs are washable (i.e., for at least 10 times of hand washes) and present photostability (i.e., daylight exposure for 7 days); all better than that of the PIFs dyed with 2-AQS, making the former one a more promising fabric material used in reusable and antibacterial/antiviral cloth face masks and protective suits for improving protection against the transmission of COVID-19 and other infectious diseases.

4. CONCLUSIONS

In this work, we present a novel approach for fabricating PIFs via chemisorption of anionic PSs on cationic cotton fabrics. The cationic cotton cloth was successfully achieved by covalently modifying the cotton with two chemical agents, DEAE-Cl or CHPTAC, respectively, and revealed potential to serve as a platform for the developments of functional textiles. The strong electrostatic interactions provided by cationic cotton with anionic RB or 2-AQS ensured sufficient adsorption capacity and washability of the photoactive agents on the materials. The resultant PIFs showcased a highly efficient biocidal effect against bacteria (e.g., *E. coli* and *L. innocua*) and a surrogate of viruses (T7 bacteriophage) with microorganism reduction rates around 5−6 logs under daylight treatment no longer than 60 min. Moreover, the presence of polycationic short chains on the polyDEAE@cotton further facilitated the biocidal functions by providing the same electrostatic affinity to microorganisms. On the other hand, the PIFs dyed with RB showed excellent washability (up to 10 times of hand wash) and photostability. This work is expected to provide a technology that can produce different innovative functional textiles for PPE developments.

https://dx.doi.org/10.1021/acsami.0c15540
ACS Appl. Mater. Interfaces 2020, 12, 49442−49451

■ ASSOCIATED CONTENT

Supporting Information

The Supporting Information is available free of charge at https://pubs.acs.org/doi/10.1021/acsami.0c15540.

Detailed procedures of antiviral tests against T7 bacteriophage; modification schemes of cotton fiber with DEAE-Cl and CHPTAC; structural characterizations of PIFs; Gaussian calculated molecular orbitals of RB and 2-AQS; and biocidal functions of PIFs against gram-positive and gram-negative bacteria under dark conditions (PDF)

■ AUTHOR INFORMATION

Corresponding Author

Gang Sun − *Agricultural and Environmental Chemistry Graduate Group and Department of Biological and Agricultural Engineering, University of California, Davis, California 95616, United States;* orcid.org/0000-0002-6608-9971; Phone: +1 530 752 0840; Email: gysun@ucdavis.edu

Authors

Peixin Tang − *Agricultural and Environmental Chemistry Graduate Group and Department of Biological and Agricultural Engineering, University of California, Davis, California 95616, United States;* orcid.org/0000-0003-3192-986X

Zheng Zhang − *Agricultural and Environmental Chemistry Graduate Group and Department of Biological and Agricultural Engineering, University of California, Davis, California 95616, United States;* orcid.org/0000-0003-0887-5859

Ahmed Y El-Moghazy − *Department of Food Science and Technology, University of California, Davis, California 95616, United States;* orcid.org/0000-0002-5743-7305

Nicharee Wisuthiphaet − *Department of Food Science and Technology, University of California, Davis, California 95616, United States*

Nitin Nitin − *Department of Biological and Agricultural Engineering and Department of Food Science and Technology, University of California, Davis, California 95616, United States*

Complete contact information is available at: https://pubs.acs.org/10.1021/acsami.0c15540

Author Contributions

P.T., Z.Z., and G.S. conceived and designed the research. P.T. and Z.Z. carried out the experiments, including PIF fabrications, PIF characterizations, ROS measurements, and antibacterial tests. A.Y.E.-M., N.W., and N.N. performed antiviral tests. P.T. and G.S. wrote and revised the manuscript. All authors have given approval to the final version of the manuscript.

Notes

The authors declare no competing financial interest.

■ ACKNOWLEDGMENTS

This work is partially supported by the COVID-19 Research Accelerator Funding Track Program (fund source number 19933) at the University of California, Davis, CA, USA. The authors are grateful for funding from the California Department of Pesticide Regulation (18-C0012). The authors would like to thank the Advanced Material Characterization and Testing Lab (AMCaT) at the University of California, Davis, for performing the SEM imaging.

■ REFERENCES

(1) Metcalf, C. J. E.; Lessler, J. Opportunities and Challenges in Modeling Emerging Infectious Diseases. *Science* **2017**, *357*, 149−152.

(2) Belongia, E. A.; Osterholm, M. T. COVID-19 and Flu, a Perfect Storm. *Science* **2020**, *368*, 1163.

(3) World Health Organization. *Coronavirus disease 2019 (COVID-19). Situation Report-197. Updated August 04, 2020.* Available at: https://www.who.int/docs/default-source/coronaviruse/situation-reports/20200804-covid-19-sitrep-197.pdf?sfvrsn=94f7a01d_2. Accessed August 04, 2020.

(4) Gralton, J.; McLaws, M. L. Protecting Healthcare Workers from Pandemic Influenza: N95 or Surgical Masks? *Crit. Care Med.* **2010**, *38*, 657−667.

(5) Eikenberry, S. E.; Mancuso, M.; Iboi, E.; Phan, T.; Eikenberry, K.; Kuang, Y.; Kostelich, E.; Gumel, A. B. To Mask or Not to Mask: Modeling the Potential for Face Mask Use by the General Public to Curtail the COVID-19 pandemic. *Infect. Dis. Model.* **2020**, *5*, 293−308.

(6) Cheng, V. C. C.; Wong, S. C.; Chuang, V. W. M.; So, S. Y. C.; Chen, J. H. K.; Sridhar, S.; To, K. K. W.; Chan, J. F. W.; Hung, I. F. N.; Ho, P. L.; Yuen, K. Y. The Role of Community-Wide Wearing of Face Mask for Control of Coronavirus Disease 2019 (COVID-19) Epidemic Due to SARS-CoV-2. *J. Infect.* **2020**, *81*, 107−114.

(7) Liao, L.; Xiao, W.; Zhao, M.; Yu, X.; Wang, H.; Wang, Q.; Chu, S.; Cui, Y. Can N95 Respirators Be Reused after Disinfection? How Many Times? *ACS Nano* **2020**, *14*, 6348−6356.

(8) Centers for Disease Control and Prevention, *CDC calls on Americans to wear masks to prevent COVID-19 spread*. Available at: https://www.cdc.gov/media/releases/2020/p0714-americans-to-wear-masks.html. Accessed July 14, 2020.

(9) Konda, A.; Prakash, A.; Moss, G. A.; Schmoldt, M.; Grant, G. D.; Guha, S. Aerosol Filtration Efficiency of Common Fabrics Used in Respiratory Cloth Masks. *ACS Nano* **2020**, *14*, 6339−6347.

(10) Zangmeister, C. D.; Radney, J. G.; Vicenzi, E. P.; Weaver, J. L. Filtration Efficiencies of Nanoscale Aerosol by Cloth Mask Materials Used to Slow the Spread of SARS CoV-2. *ACS Nano* **2020**, *14*, 9188−9200.

(11) Ma, Y.; Li, J.; Si, Y.; Huang, K.; Nitin, N.; Sun, G. Rechargeable Antibacterial N-Halamine Films with Antifouling Function for Food Packaging Applications. *ACS Appl. Mater. Interfaces* **2019**, *11*, 17814−17822.

(12) Huang, C.; Chen, Y.; Sun, G.; Yan, K. Disinfectant Performance of a Chlorine Regenerable Antibacterial Microfiber Fabric as a Reusable Wiper. *Materials (Basel).* **2019**, *12*, 127.

(13) Si, Y.; Li, J.; Zhao, C.; Deng, Y.; Ma, Y.; Wang, D.; Sun, G. Biocidal and Rechargeable N-Halamine Nanofibrous Membranes for Highly Efficient Water Disinfection. *ACS Biomater. Sci. Eng.* **2017**, *3*, 854−862.

(14) Zhong, H.; Zhu, Z.; You, P.; Lin, J.; Cheung, C. F.; Lu, V. L.; Yan, F.; Chan, C. Y.; Li, G. Plasmonic and Superhydrophobic Self-Decontaminating N95 Respirators. *ACS Nano* **2020**, *14*, 8846−8854.

(15) Si, Y.; Zhang, Z.; Wu, W.; Fu, Q.; Huang, K.; Nitin, N.; Ding, B.; Sun, G. Daylight-Driven Rechargeable Antibacterial and Antiviral Nanofibrous Membranes for Bioprotective Applications. *Sci. Adv.* **2018**, *4*, No. eaar5931.

(16) Liu, N.; Sun, G.; Zhu, J. Photo-Induced Self-Cleaning Functions on 2-Anthraquinone Carboxylic Acid Treated Cotton Fabrics. *J. Mater. Chem.* **2011**, *21*, 15383−15390.

(17) Zhuo, J.; Sun, G. Antimicrobial Functions on Cellulose Materials Introduced by Anthraquinone Vat Dyes. *ACS Appl. Mater. Interfaces* **2013**, *5*, 10830−10835.

(18) Chen, W.; Chen, J.; Li, L.; Wang, X.; Wei, Q.; Ghiladi, R. A.; Wang, Q. Wool/Acrylic Blended Fabrics as Next-Generation Photodynamic Antimicrobial Materials. *ACS Appl. Mater. Interfaces* **2019**, *11*, 29557−29568.

(19) Tang, P.; Zhang, M.; Robinson, H.; Sun, G. Fabrication of Robust Functional Poly-Cationic Nanodots on Surfaces of Nucleophilic Nanofibrous Membrane. *Appl. Surf. Sci.* **2020**, *528*, 146587.

(20) Tang, P.; Sun, G. Generation of Hydroxyl Radicals and Effective Whitening of Cotton Fabrics by H2O2 under UVB Irradiation. *Carbohydr. Polym.* **2017**, *160*, 153−162.
(21) Zhang, Z.; Si, Y.; Sun, G. Photoactivities of Vitamin K Derivatives and Potential Applications as Daylight-Activated Antimicrobial Agents. *ACS Sustainable Chem. Eng.* **2019**, *7*, 18493−18504.
(22) Zhang, Z.; El-Moghazy, A.; Wisuthiphaet, N.; Nitin, N.; Castillo, D.; Murphy, B.; Sun, G. *Daylight-Induced Antibacterial and Antiviral Nanofibrous Membranes Containing Vitamin K Derivatives for Personal Protective Equipment*. Submitted to ACS Appl. Mater. Interfaces 2020.
(23) Liu, N.; Sun, G. Production of Reactive Oxygen Species by Photoactive Anthraquinone Compounds and Their Applications in Wastewater Treatment. *Ind. Eng. Chem. Res.* **2011**, *50*, 5326−5333.
(24) Planas, O.; Macia, N.; Agut, M.; Nonell, S.; Heyne, B. Distance-Dependent Plasmon-Enhanced Singlet Oxygen Production and Emission for Bacterial Inactivation. *J. Am. Chem. Soc.* **2016**, *138*, 2762−2768.
(25) Wiehe, A.; O'Brien, J. M.; Senge, M. O. Trends and Targets in Antiviral Phototherapy. *Photochem. Photobiol. Sci.* **2019**, *18*, 2565−2612.
(26) Fang, F. C. Antimicrobial Reactive Oxygen and Nitrogen Species: Concepts and Controversies. *Nat. Rev. Microbiol.* **2004**, *2*, 820−832.
(27) Pan, X.; Zhou, G.; Wu, J.; Bian, G.; Lu, P.; Raikhel, A. S.; Xi, Z. Wolbachia Induces Reactive Oxygen Species (ROS)-Dependent Activation of the Toll Pathway to Control Dengue Virus in the Mosquito Aedes Aegypti. *Proc. Natl. Acad. Sci. U. S. A.* **2012**, *109*, E23−E31.
(28) Fu, S.; Hinks, D.; Hauser, P.; Ankeny, M. High Efficiency Ultra-Deep Dyeing of Cotton via Mercerization and Cationization. *Cellulose* **2013**, *20*, 3101−3110.
(29) Terada, A.; Okuyama, K.; Nishikawa, M.; Tsuneda, S.; Hosomi, M. The Effect of Surface Charge Property on Escherichia Coli Initial Adhesion and Subsequent Biofilm Formation. *Biotechnol. Bioeng.* **2012**, *109*, 1745−1754.
(30) Mi, X.; Bromley, E. K.; Joshi, P. U.; Long, F.; Heldt, C. L. Virus Isoelectric Point Determination Using Single-Particle Chemical Force Microscopy. *Langmuir* **2020**, *36*, 370−378.
(31) Xu, Y.; Takai, M.; Ishihara, K. Protein Adsorption and Cell Adhesion on Cationic, Neutral, and Anionic 2-Methacryloyloxyethyl Phosphorylcholine Copolymer Surfaces. *Biomaterials* **2009**, *30*, 4930−4938.
(32) Kaur, R.; Anastasio, C. Light Absorption and the Photoformation of Hydroxyl Radical and Singlet Oxygen in Fog Waters. *Atmos. Environ.* **2017**, *164*, 387−397.
(33) *Launder-O-Meter AATCC Test Method 61−1996 Colorfastness to Laundering, Home and Commercial: Accelerated*, available at: https://csbs.uni.edu/sites/default/files/Launderometer.pdf.

https://dx.doi.org/10.1021/acsami.0c15540
ACS Appl. Mater. Interfaces 2020, 12, 49442−49451